AIAA 81-4009

Measurements of Wavenumber-Celerity Spectrum in Plane and Axisymmetric Jets

A. K. M. F. Hussain* and A. R. Clark†
University of Houston, Houston, Texas

The wavenumber-convection velocity spectra $W(k,U)$ in the near and far fields of plane and axisymmetric free air jets have been computed from digitized hot-wire data. This spectrum, which is the double Fourier-transformation of the space-time correlation $R(s,\tau)$ was obtained in a 3.18 × 140 cm plane jet and in a 2.54-cm-diam axisymmetric jet. For both jets the exit mean velocity $\bar{U}_e$ was 30 m/s. The reference (upstream) probe was located at $x/d=8$ for the near-field data and at $x/d=30$ for the far-field data, d denoting the exit diameter or slit width. The spectra indicate that the jets are characterized by energetic large-scale structures not only in the near field (slightly downstream of the potential core) but also in the self-preserving region. The streamwise length scale of the most energetic eddies increases in proportion with that of the jet width. The streamwise length scale of these eddies is about 3 times the local jet width in the circular jet and 3.5 times the local jet width in the plane jet. The convection velocity U of the dominant eddies decreases from about $0.8\bar{U}_e$ to $0.5\bar{U}_e$ between the two regions in the plane jet and from about $0.73\bar{U}_e$ to $0.25\bar{U}_e$ between the two regions in the axisymmetric jet. With increasing eddy sizes, the dispersion in the convection velocity U increases as $W(k,U)$ becomes progressively skewed towards U values higher than the local time mean velocity $\bar{U}$.

Introduction

THE time-average space-time correlation $R(s,\tau)$ has been used extensively to infer convection velocities of coherent vortical fluid parcels or eddies in turbulent shear flows; here s is the spatial separation between the sensors in the streamwise direction and τ is the time delay between their signals. Unfortunately, interpretations from time-average correlation data $R(s,\tau)$ are fraught with some constraints. One such constraint is the lack of uniqueness of the results. For example, the structure convection velocity that can be inferred from the correlation contours is not unique. The three most commonly used convection velocities U_s, U_τ, and U_R are defined by the $R(s,\tau)=$const contour in the (s,τ) plane as follows:

1) $U_s \equiv s_1/\tau_p$, where $\tau=\tau_p$ is the time delay corresponding to the peak value of $R(s_1,\tau)$ at each given streamwise separation $s=s_1$; τ_p is identified such that $\partial R(s_1,\tau)/\partial\tau=0$.

2) $U_\tau \equiv s_p/\tau_1$, where $s=s_p$ is the separation corresponding to the peak value of $R(s,\tau_1)$ for each time delay $\tau=\tau_1$; s_p is identified such that $\partial R(s,\tau_1)/\partial s=0$.

3) $U_R \equiv s'/\tau'$ where (s',τ') are the coordinates of the intersection of an $R(s,\tau)=$const ellipse-like contour with its major axis.

In general, $U_s \geq U_R \geq U_\tau$. In the studies of aerodynamic noise and other wave phenomena, since the optimum time scale (rather than the optimum length scale) is more relevant,[1] U_τ typically has been used.[2-4] It should be noted that three additional convection velocities U_s', U_τ', $U_{s\tau}'$ can be identified.[5,6] These are defined as:

4) $U_s' \equiv \partial s/\partial\tau$ of the loci connecting the points where $\partial R(s,\tau)/\partial\tau=0$.

5) $U_\tau' \equiv \partial s/\partial\tau$ of the loci connecting the points where $\partial R(s,\tau)/\partial s=0$.

6) $U_{s\tau}' \equiv (U_s U_\tau)^{1/2}$.

The convection velocities U_s, U_τ, U_R, U_s' and U_τ' are schematically represented in Fig. 1a.

Note that when the correlation contours are like those shown in Fig. 1b, all the six convection velocities are identical. This should be expected to occur in homogeneous turbulence when the turbulence is essentially "frozen" and advected downstream at the time-mean velocity U_∞. Favre et al.[5] experimentally showed this to be true. For turbulent shear flows, however, the $R=$const contours have been seen to be more like those in Fig. 1a. Only at large separations should the contours look progressively like those in Fig. 1b.

In addition to the variety of convection velocities defined above, there is a second source of ambiguity. The measured convection velocity on the basis of any of the above definitions also depends on the value of s or τ used in the measurement. For example, since only large eddies survive for long enough to contribute to correlations measured with large probe separations, the average convection velocity inferred from such correlation measurements would be weighted by the larger, energetic eddies. Furthermore, the s-dependence of U_s and the τ-dependence of U_τ may be different. Favre et al.[5] showed that, while U_s was practically independent of the probe separations, U_τ varied strongly with the time delay τ.

Another constraint regarding the inference of convection velocity from space-time correlation measurements is that the measured convection velocity is a weighted average of the convection velocities of the various sized eddies. Flow visualization has shown that a turbulent shear flow consists of eddies of a wide range of length scales which convect with velocities varying over a wide range—both above and below the local time-mean velocity. Clearly, an understanding of the dependence of the convection velocity on the eddy size is desirable. Some researchers have attempted to determine this dependence via narrowband frequency filtered space-time correlation measurements. This approach, however, has the limitation that the filter is sensitive only to the time-frequency and thus *cannot* discriminate between a large eddy moving rapidly and a small eddy moving slowly.

Wills[7] appears to be the first to have suggested that by considering the turbulent shear flow as a superposition of harmonic travelling waves, the space-time correlation $R(s,\tau)$ can be Fourier-transformed in both s and τ to obtain the wavenumber-frequency spectrum $M(k,f)$. Since for a wave of wavenumber k, the convection velocity U is f/k, the wavenumber-convection velocity spectrum $W(k,U)$ can be

Received Dec. 27, 1979; revision received May 12, 1980.

*Professor, Associate Fellow AIAA.

†Graduate Student, Dept. of Mechanical Engineering; presently Research and Development, ARCO Oil and Gas Company.

defined as $W(k,U)=M(k,f/k)$. Thus,

$$M(k,f)=\int\int_{-\infty}^{\infty} R(s,\tau)\exp[-j2\pi(ks+f\tau)]\,ds\,d\tau$$

$$=\int_{-\infty}^{\infty} G(s,f)\exp[-j2\pi ks]\,ds$$

where

$$G(s,f)=C(s,f)-jQ(s,f)$$

Willis[7] measured $C(s,f)$ for the single reference probe location $(x/D,y/D)=(2,0.5)$ in the axisymmetric mixing layer of a small jet. The measurements were made for a few (broad) bandpass center frequencies using a ⅓-octave analyzer. He then obtained $W(k,U)$ data by neglecting the quadrature spectrum $Q(s,f)$.

This brief paper presents our $W(k,U)$ data taken in the near and far fields of plane and axisymmetric jets employing high-resolution digital data acquisition and analysis. The approach differs from that of Wills in that the digitized hot wire data from two hot-wires separated in the streamwise direction (which have not been bandpass filtered) have been digitally Fourier-transformed directly in time to obtain the complete spectrum $G=C-jQ$ from which the complete wavenumber-celerity spectrum $W(k,U)$ has been computed.

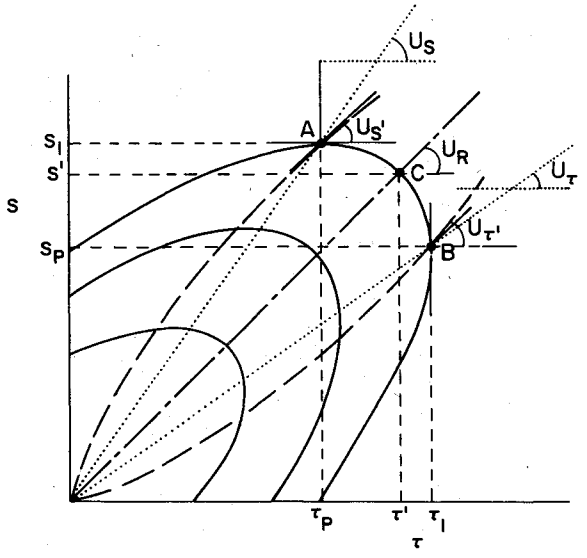

Fig. 1a Convection velocity definitions based upon $R(s,\tau)$ contours in (s,τ) plane defining U_s', U_τ', U_s, U_τ, and U_R.

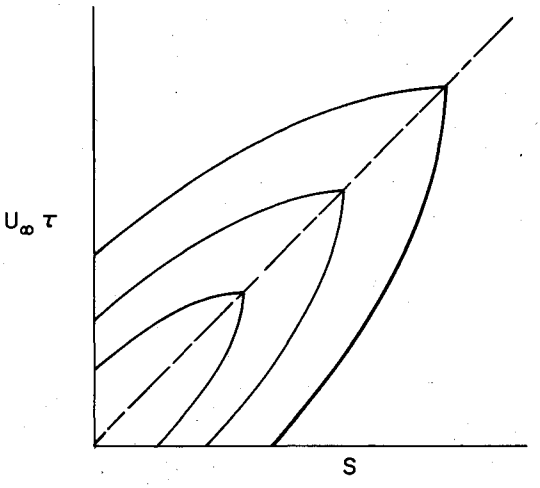

Fig. 1b Correlation contours for which $U_s=U_\tau=U_R=U_s'=U_\tau'$.

Apparatus

The experiments were carried out in a plane jet facility and a circular jet facility located in a large laboratory having controlled temperature, humidity, and traffic. The automated probe traverse and data acquisition/analysis were performed on-line under the remote control of the laboratory computer (HP 2100S) located in an adjoining room. Thus, the jet flows, run one at a time, are free from significant ambient recirculation and turbulence[8,9] and operator-induced disturbances. The plane jet emerges through a 3.18×140 cm vertical slit (aspect ratio 44:1) following a 44:1 two-dimensional (cubic equation profile) contraction. The slit is located at the middle of a 140×200 cm end plate which is provided with rounded leading edges for preventing separation of the entrainment-induced boundary layer on the end plate. The jet is bounded between a top and a bottom confining plates of size 200×360 cm. The exit flow is homogeneous in the spanwise direction. The 2.54-cm axisymmetric jet emerges through the center of a 30-cm-diam end plate following a 100:1 axisymmetric (Batchelor-Shaw) contraction. The facility consists of two settling chambers in tandem, the first chamber attached with a loudspeaker for our related study of controlled excitation of the axisymmetric jet.[10] The second settling chamber helps to assure axisymmetry of the jet, as confirmed by congruence of mean velocity and fluctuation intensity profiles measured near the exit in several azimuthal planes.

Both of the facilities consist of separate modules connected together through flexible couplings. The motor-blower assembly in each case is mounted on a platform having no rigid connection with the rest of the tunnel. The nozzles are free from any perceptible vibration. Each facility is driven by a full-wave rectifier-controlled dc motor which can hold the jet speed constant over a long period.

For each jet the exit freestream values of the mean velocity U_e and longitudinal fluctuation intensity were 30 m/s and 0.3%. The mean velocity profiles and the shape factors of the laminar exit boundary layers compared well with the Blasius profile. Further details of the facilities and flow documentation are available in Refs. 10 and 11.

The data were taken using 3.8-μm-diam, 2-mm-long tungsten hot wires operated (at an overheat ratio of 0.5) by linearized DISA constant temperature anemometers (models 55M and 55D10).

Procedure

Data were obtained simultaneously from two single hot wires, the upstream (reference) wire located at the reference station, viz., $x/d=8$ or 30, and the downstream wire progressively traversed in the streamwise direction. At each separation, correlation between the two signals was obtained on-line. The choices of these two reference locations were dictated by the desire to obtain the $W(k,U)$ data in the near and far fields of the jets. Although the jets are unlikely to achieve self-preservation completely at $x/d=30$, it was felt that this region was far enough from the origin of the jet to essentially represent the time-average characteristic features of the self-preserving region. At distances farther downstream, the velocity signals would be too weak to neglect the effects of ambient turbulence and circulation. For the near-field data, it was decided that the region of measurement should start as far upstream as possible. However, in order for the data to represent jet flow, measurements had to be taken downstream from the potential core. Even though time-averaged centerline velocity $\bar{U}_c$ data suggest that the potential

core ends at $x/d \cong 4.5$, the potential core indeed persists much farther. The core potential fluid is bounded by the turbulent mixing layer vortical structures whose lateral wandering produces a time-mean U_c smaller than the exit velocity $\bar{U}_e$, before the core fluid is completely entrained by the vortical fluid in the axisymmetric mixing layer. Our studies suggest that entrainment of core fluid is complete at $x/d \cong 8$; hence the choice of the upstream reference location.

The probe traverses were made using backlash-free traversing mechanisms driven by computer-controlled stepping motors. The two probes approached the streamwise line from opposite sides of the jet at an angle to the jet axis so as to minimize the probe interference. A small transverse displacement $\Delta y = 0.8$ mm was provided between the two hot wires to eliminate wake effects on the downstream probe at small streamwise separations. For a number of separations, the mean velocity $\bar{U}$, rms fluctuation u', and frequency spectra measured at the downstream probe—both with and without the upstream probe in place—were found to be indistinguishable.

The two linearized hot-wire signals were first bandpass filtered (consistent with the Nyquist sampling criterion and the ensemble record length requirement) before being digitized by the 12-bit A/D converter. Eighth-order analog filters (Krohn-Hite model 3341 with 48 dB/octave roll-off) were used for this purpose. After filtering, the signals were amplified prior to digitization so that the full range (-2048 to $+2047$ count) of the A/D converter could be utilized. The near-field signals were sampled at 6400 samples/s, while the far-field signals were sampled at 1600 samples/s.

A total of 64 probe separations was used providing a spatial resolution $\Delta s = s_{max}/64$, s_{max} being the maximum probe separation. The s_{max} values were selected to match the largest wavelengths expected, consistent with the low-frequency cutoff of the filters and the estimated large-scale convection velocities over the ranges of measurement.

At each probe separation s, the ensemble-averaged complex function $G(s,f)$ was calculated from 200 individual spectral estimates. Prior to computing each estimate, the digitized time series derived from ac-coupled hot wire signals were tapered with the cosine window function, and then fast Fourier-transformed using a high-speed microcoded FFT subroutine.

The ensemble averaged function $G(s,f) = C(s,f) - jQ(s,f)$ was frequency-smoothed prior to Fourier-transforming in s to obtain $M(k,f)$. An assembly language discrete Fourier transform routine was used for this purpose. For further details of the data acquisition and analysis, see Ref. 12.

Results and Discussion

Data have been obtained for three reference locations in the plane jet and two reference locations in the axisymmetric jet. The wavenumber-celerity spectra $W(k,U)$ corresponding to these points are shown in Figs. 2-6 in the form of contours of constant values of W in the (k,U) plane. Spectral levels of W ranging from 1 to 90% of the local maximum W_{max} are represented. Also shown is the mean velocity $\bar{U}_r$ at each reference point. Since the velocity and length scales differ at the various reference points, the coordinate axes have been left dimensional.

At each wavenumber, there is a large dispersion in the convection velocity, i.e., an eddy can convect with a convection velocity over a wide range. We can define $U_c(k)$ to be the most probable convection velocity, i.e., U_c is the value of U at which $W(k,U)$ has a maximum. Note that in Figs. 2-6, the locus $U_c(k)$ corresponds to the condition where $\partial W(k,U)/\partial U = 0$.

Figure 2 shows the isoenergy contours for the plane jet with the reference probe located on the centerline at $x/d = 8$. For this case the local centerline velocity $\bar{U}_r$ is 27 m/s (which equals 0.9 $\bar{U}_e$). Note that the peak energy occurs at $k_d \cong 0.075$ cm^{-1} and $U_d = 25$ m/s, these being the wavenumber

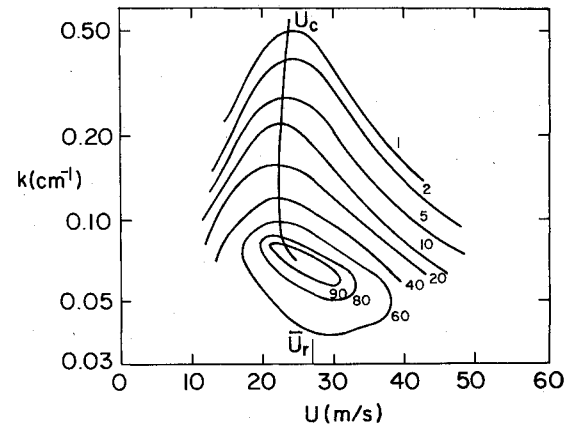

Fig. 2 Contours of spectrum $W(k,U)$ as percentages of W_{max} in the plane jet with reference probe at $x/d = 8$, $y/d = 0$; $\bar{U}_r = 27$ m/s.

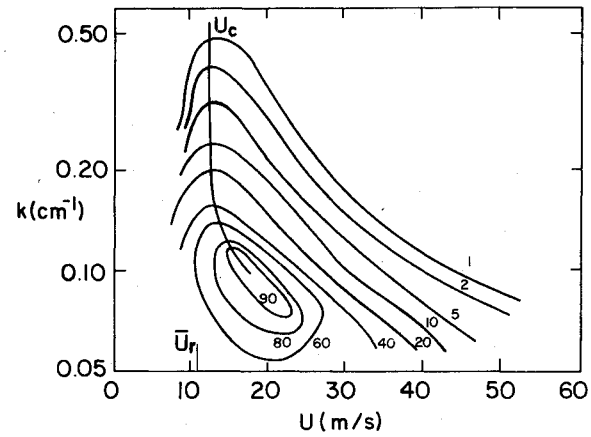

Fig. 3 Contours of spectrum $W(k,U)$ as percentages of W_{max} in plane jet with reference probe at $x/d = 8$, at transverse location where $\bar{U}/\bar{U}_m = 0.4$; $\bar{U}_r = 10.8$ m/s.

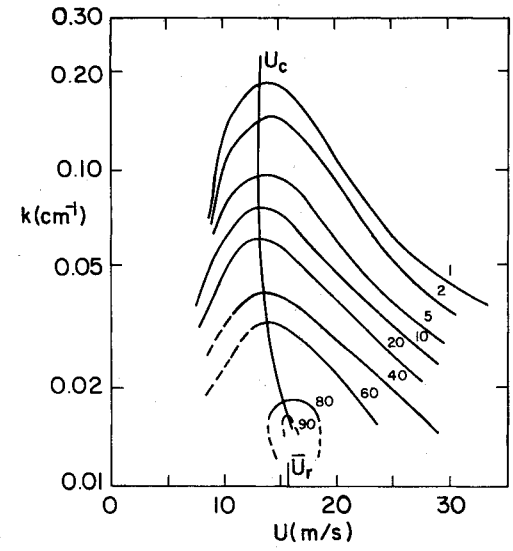

Fig. 4 Contours of spectrum $W(k,U)$ as percentages of W_{max} in plane jet with reference probe at $x/d = 30$, $y/d = 0$; $\bar{U}_r = 15.3$ m/s.

and convection velocities of the most energetic or dominant scale; the subscript d denotes the most (energetic) dominant eddy. Note that for sizes smaller than $L_d (\equiv k_d^{-1})$, the contours are essentially symmetric, whereas for $k < k_d$ they are highly skewed toward larger U. This appears to be the essential trend with all other cases (in Figs. 3-6). At large k, U_c gradually approaches $\bar{U}_r$, consistent with the expectation

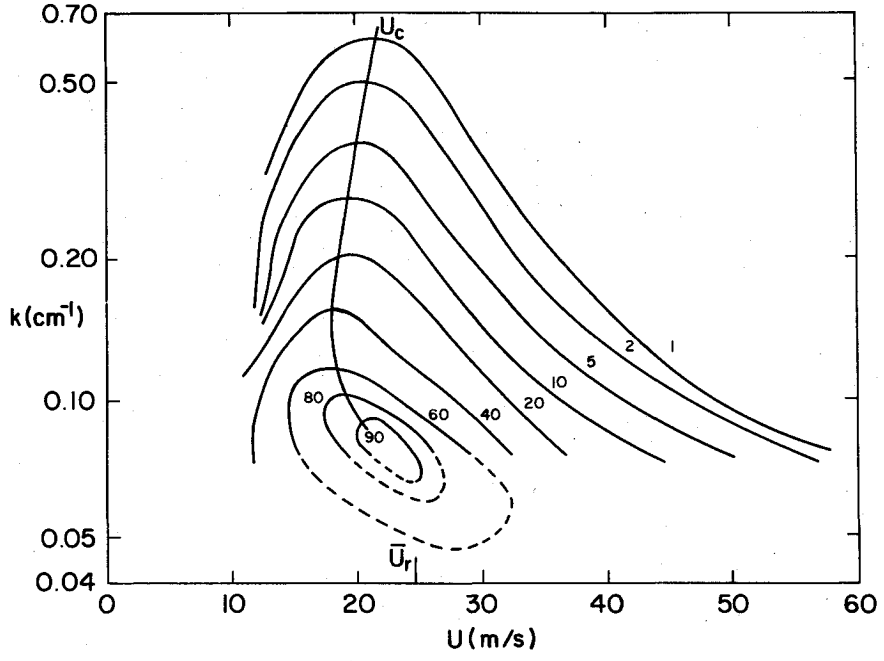

Fig. 5 Contours of spectrum $W(k,U)$ as percentages of W_{max} in circular jet with reference probe at $x/d=8$, $y/d=0$; $\bar{U}_r=24$ m/s.

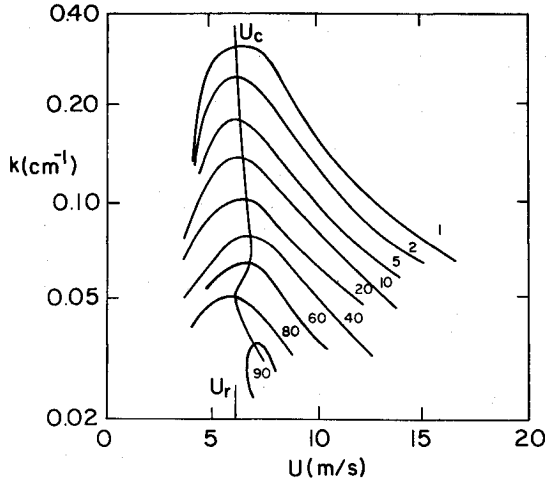

Fig. 6 Contours of spectrum $W(k,U)$ as percentages of W_{max} in circular jet with reference probe at $x/d=30$, $y/d=0$; $\bar{U}_r=6$ m/s.

that the smallest eddies are likely to be convected with a velocity nearly equal to the local time-mean flow velocity. Note that the eddies of size $k\cong 0.1$ cm^{-1} have the minimum value of U_c.

In order to obtain some understanding of the transverse variation of the convection velocity and the dominant length scale, data were also obtained with the reference probe at $x/d=8$, but on one side of the jet, i.e., at the transverse location where the local mean velocity $\bar{U}$ equals 40% of the centerline velocity $\bar{U}_m$ at the same station. These data are shown in Fig. 3. Note that the local velocity $\bar{U}_r=10.8$ m/s $=0.36\,\bar{U}_e$, which is 40% of local maximum mean velocity $\bar{U}_m=27$ m/s. Note that the convection velocity U_d of the most energetic scale is about 18 m/s and that $k_d\cong 0.09$ cm^{-1}. The value of U_d at this location is about 72% of the centerline value at the same x. On the outer edge of a jet, the hot-wire senses the "footprints" of the structures in the jet and thus would give a dominant convection velocity which is not necessarily that of the eddies passing by the probe. Rather, the convection velocity will be weighted by the energetic eddies on the jet center, primarily through potential motions induced by the eddies. That is why U_d is considerably larger than the local mean velocity which, when averaged over the streamwise distance between the two probes, is even lower than $\bar{U}_r=10.8$ m/s. The smallest eddies generally will be advected with a convection velocity equal to the local time mean velocity. Thus, U_c for $(k\to\infty)$ should nearly approach $\bar{U}_r$. Note that since data along $\bar{U}/\bar{U}_m=0.4$ are dominated by large-scale structures in the jet center, τ_d at this location is essentially the same as that on the centerline. Note that the $U_c(k)$ variations in Fig. 3 do not have a minimum as in Fig. 2. At the smallest scales, the convection velocity range is narrower. The $W(k,U)$ contours are most skewed toward higher U at an outer layer of the jet than on the jet centerline. The dominant scale Strouhal number $St_d=f_d d/\bar{U}_e$ is about 0.18 for both Figs. 2 and 3, a result consistent with the controlled excitation study of Hussain and Thompson[13] in the same jet.

Figure 4 shows isoenergy contours measured in the far field of the plane jet. The reference probe was located on the centerline at $x/d=30$, corresponding to $\bar{U}_r=0.51\,\bar{U}_e$. Note that the dominant eddy size $L_d=k_d^{-1}$ is about 21 d, which represents nearly a fourfold increase from the near-field station value of 4.8 d. Earlier data[11] showed that the time-mean jet width b increases with x approximately as $b/d=0.23\,(x/d-2)$; the jet widths at $x/d=8$ and 30 would be roughly 1.4 and 6.5 d. Thus, the increase in the most energetic structure length scale L_d between $x/d=8$ and $x/d=30$ is in the same ratio as that of the time-mean jet width. These variations appear reasonable and thus provide additional confidence in the present data analysis technique.

$W(k,U)$ contours for the near field of the axisymmetric jet are shown in Fig. 5; the reference probe was located on the centerline at $x/d=8$ where $\bar{U}_r=0.8\,\bar{U}_e$. Figure 6 shows the far-field $W(k,U)$ data with the reference probe located on the centerline at $x/d=30$; at this point $\bar{U}_r=0.2\,\bar{U}_e$. At $x/d=8$, the variation of $U_c(k)$ is smooth, with a minimum occurring near $W/W_{max}=0.5$. At the larger x/d, the contours are narrower at higher k. Note that the local minimum in $U_c(k)$ appearing as a hump at $W=0.8\,W_{max}$ in Fig. 6 is characteristic of the flow and not an experimental error. The length scale L_d of the most energetic scale at $x/d=8$ and 30 is roughly 5 and 15 d, respectively. Since for the circular jet the jet spread is given as $b/d=0.176\,(x/d+1.3)$, the jet widths at $x/d=8$ and 30 should be 1.63 and 5.41 d. Thus, as for the plane jet, the increase in L_d in the downstream direction is, as expected, proportional to the increase in jet width.

Concluding Remarks

Following the analytical suggestions of Wills,[7] the wavenumber-celerity spectra were measured in the near and far fields of an axisymmetric jet and a high-aspect-ratio plane jet. The measurement method was different from that of Wills in that the complete complex spectrum was obtained by double Fourier transformation of digitized hot-wire signals.

The nature of the $W(k,U)$ contours suggests that both the near and far fields of plane and axisymmetric jets are characterized by eddies advecting downstream. The distinct peak in the $W(k,U)$ contour in each case suggests occurrence of a dominant scale of the eddies. The wavenumber k_d and the convection velocity U_d of the most energetic eddies are identified by the peak in the $W(k,U)$ contour.

This method of analysis of shear flow turbulence, even though does not reveal the details of the coherent structures, provides statistics of the most energetic eddy and of the range and distribution of its convection velocity. Note that at each length scale or eddy size, there is a range of the convection velocity U with which the eddies of the same size travel downstream. The dispersion in U increases with increasing eddy size. The predominant convection velocity at each wavenumber is given by U_c. (For a discussion of frequency-dependent convection velocities in turbulent shear flows, see Refs. 14 and 15.) The smallest eddies are essentially transported passively so that the range of their convection velocity is expected to be small and approach the local time mean velocity as $k\to\infty$. Note that in each of Figs. 2-6, U_c approaches $\bar{U}_r$ as $k\to\infty$. By contrast, the larger eddies are not passively advected but undergo large excursions in their convection velocities due to interactions with other structures. Flow visualization movies in a high Reynolds number mixing layer[12] have shown a wide range of the convection velocity of large-scale structures—ranging from a fraction of the local time-mean velocity $\bar{U}$ to values significantly higher than $\bar{U}$. In a controlled excitation study,[10] convection velocities of the large-scale coherent structures in the mixing layer of a circular jet showed a variation between 0.4 and 1.25 $\bar{U}_e$. (Note that even in a laminar shear layer, the convection velocity can exceed the local maximum velocity.[17])

On the centerline of a jet, eddies of a particular size may have convection velocities higher or lower than the local time-mean velocity. However, closer to the outer edge, most eddies are likely to arrive from the jet center. Thus, energy spectrum distribution in U is likely to be more skewed toward higher U, and U_c is more likely to be higher than $\bar{U}_r$.

The distribution of the spectra $W(k,U)$ in the wavenumber range suggests that even though the energy content increases with increasing size, there is an optimum size (k_d^{-1}) where the energy density is the maximum. Still larger eddies exist, and the fact that their total energy for any eddy size is lower does not imply that these are individually weaker, but that these are less numerous.

The streamwise length scale of the most energetic eddies increases in proportion with the jet width. For the plane jet, the most energetic eddy was found to be about 4.8 d long in the streamwise direction in the near-field region and about 21 d long in the far-field region studied. For the axisymmetric jet, the corresponding sizes were found to be about 5 and 15 d, respectively.

Acknowledgment

This research was funded by the National Science Foundation under Grant ENG 75-15226.

References

[1] Lighthill, M. J., "On Sound Generated Aerodynamically: II. Turbulence as a Source of Sound," *Proceedings of the Royal Society,* Series A, Vol. 222, 1954, pp. 1-32.

[2] Phillips, O. M., "On the Generation of Waves by Turbulent Wind," *Journal of Fluid Mechanics,* Vol. 2, 1957, pp. 417-445.

[3] Bradshaw, P., Ferriss, D. H., and Johnson, R. F., "Turbulence in the Noise Producing Region of a Circular Jet," *Journal of Fluid Mechanics,* Vol. 19, 1964, pp. 591-624.

[4] Willmarth, W. W. and Wooldridge, C. E., "Measurements of the Fluctuating Pressure Beneath a Thick Boundary Layer," *Journal of Fluid Mechanics,* Vol. 14, 1962, pp. 187-210.

[5] Favre, A., Gaviglio, J., and Dumas, R., "Structure of Velocity Space-Time Correlation in a Boundary Layer," *The Physics of Fluids Supplement,* Vol. 10, 1967, pp. S138-S144.

[6] Hinze, J. O., *Turbulence,* 2nd Ed., McGraw-Hill Book Co., New York, 1975.

[7] Wills, J. A. B., "On Convection Velocities in Turbulent Shear Flows," *Journal of Fluid Mechanics,* Vol. 20, 1964, pp. 417-432.

[8] Kotsovinos, N. E., "A Note on the Spreading Rate and Virtual Origin of a Plane Turbulent Jet," *Journal of Fluid Mechanics,* Vol. 77, 1976, pp. 305-311.

[9] Bradshaw, P., "Effect of External Disturbances on the Spreading Rate of a Plane Turbulent Jet," *Journal of Fluid Mechanics,* Vol. 80, 1977, pp. 795-797.

[10] Zaman, K. B. M. Q. and Hussain, A. K. M. F., "Vortex Pairing in a Circular Jet Under Controlled Excitation. Part 1: General Jet Response," *Journal of Fluid Mechanics,* 1980 (to be published).

[11] Hussain, A. K. M. F. and Clark, A. R., "Upstream Influence on the Near Field of a Plane Turbulent Jet," *The Physics of Fluids,* Vol. 20, 1977, pp. 1416-1426.

[12] Clark, A. R., Ph.D. Dissertation, Dept. of Mechanical Engineering, University of Houston, Texas, 1979.

[13] Hussain, A. K. M. F. and Thompson, C. A., "Controlled Symmetric Excitation of the Plane Jet: An Experimental Study of the Initial Region," *Journal of Fluid Mechanics,* Vol. 100, 1980, pp. 397-431.

[14] Heidrick, T. R., Banerjee, S., and Azad, R. S., "Experiments on the Structure of Turbulence in Fully Developed Pipe Flow: Interpretation of the Measurements by a Wave Model," *Journal of Fluid Mechanics,* Vol. 81, 1977, pp. 137-154.

[15] Bullock, K. J., Cooper, R. E., and Abernathy, F. H., "Structural Similarity in Radial Correlations and Spectra of Longitudinal Velocity Fluctuations in Pipe Flow," *Journal of Fluid Mechanics,* Vol. 88, 1978, pp. 585-608.

[16] Hussain, A. K. M. F. and Clark, A. R., "On the Coherent Structure of the Axisymmetric Mixing Layer: A Flow-Visualization Study," *Journal of Fluid Mechanics,* 1980 (to be published).

[17] Bechert, D. and Pfizenmaier, E., "On Wave-Like Perturbations in a Free Jet Travelling Faster than the Mean Flow in the Jet," *Journal of Fluid Mechanics,* Vol. 72, 1975, pp. 341-352.